Published in final edited form as:
Biochem Biophys Res Commun. 2006 May 5; 343(2): 351–360.

Nanosecond pulsed electric fields cause melanomas to self-destruct

Richard Nuccitelli[a,b,*], **Uwe Pliquett**[a], **Xinhua Chen**[a], **Wentia Ford**[a], **R. James Swanson**[a], **Stephen J. Beebe**[a,c], **Juergen F. Kolb**[a], and **Karl H. Schoenbach**[a]

a *Frank Reidy Research Center for Bioelectrics, Old Dominion University, Norfolk, VA, USA*

b *BioElectroMed Corp., Norfolk, VA, USA*

c *Eastern Virginia Medical School, Norfolk, VA, USA*

Abstract

We have discovered a new, drug-free therapy for treating solid skin tumors. Pulsed electric fields greater than 20 kV/cm with rise times of 30 ns and durations of 300 ns penetrate into the interior of tumor cells and cause tumor cell nuclei to rapidly shrink and tumor blood flow to stop. Melanomas shrink by 90% within two weeks following a cumulative field exposure time of 120 μs. A second treatment at this time can result in complete remission. This new technique provides a highly localized targeting of tumor cells with only minor effects on overlying skin. Each pulse deposits 0.2 J and 100 pulses increase the temperature of the treated region by only 3 °C, ten degrees lower than the minimum temperature for hyperthermia effects.

Keywords

Skin cancer; Cancer therapy; Tumor; Pulsed electric fields; Pyknosis; Inhibiting angiogenesis; DNA; Nucleus

Electric fields have been employed in several different types of cancer therapy. Some of these involve radiofrequency or microwave devices that heat the tumor to greater than 43 °C to kill the cells via hyperthermia [1,2]. Others use pulsed electric fields to permeabilize the tumor cells to allow the introduction of toxic drugs or DNA [3–5]. We have discovered that ultrashort electrical pulses can be used as a purely electrical cancer therapy that kills tumors without hyperthermia or drugs. Previous work from this laboratory found that fibrosarcoma tumors treated in vivo with ten 300 ns pulses exhibited a reduced growth rate compared to control tumors in the same animal [6]. Here, we report that when melanoma tumors are treated with four hundred of these pulses, tumors shrink by 90% within two weeks and a subsequent treatment can result in complete remission.

The main characteristics of these nanosecond pulsed electric fields (nsPEF) are their low energy that leads to very little heat production and their ability to penetrate into the cell to permeabilize intracellular organelles [7,8] and release calcium [9–11] from the endoplasmic reticulum [11]. They provide a new approach for physically targeting intracellular organelles with many applications, including the initiation of apoptosis in cultured cells [12–14] and tumors [6], enhancement of gene transfection efficiency [13,14], and inhibiting tumor growth [6]. During the past year, we have treated over 300 murine melanomas in 120 mice with 40 kV/cm electric field pulses 300 ns in duration with dramatic results. Every tumor exposed to 400 such pulses exhibits rapid pyknosis and reduced blood flow and shrinks by an average of 90% within two

* Corresponding author. Fax: +1 757 314 2397. *E-mail address:*rnuccite@odu.edu (R. Nuccitelli)..

weeks. A second treatment of 300 pulses can completely eliminate the melanoma. This very short total field exposure time of only 210 μs stimulates melanomas to self-destruct without drugs or significant side effects. How do these nanosecond pulsed electric fields penetrate into the cell and have such dramatic effects?

The efficacy of this nsPEF treatment depends on two separate electric field parameters: pulse duration and amplitude. The effect of pulse duration can be understood by considering the process of membrane charging when the cell is placed in an electric field. Ions in the cell interior will respond to the electric field by moving in the field direction and charging the highly resistive membrane until they experience no further force. By definition this will only occur when their redistribution establishes an equal and opposite field so that the net electric field in the cell interior is zero. However, this redistribution takes a certain amount of time that is characterized by the charging time constant of the plasma membrane, typically in the 0.1–1μs range. If the nsPEF is shorter than this charging time, the interior charges will not have sufficient time to redistribute to counteract the imposed field and it will penetrate into the cell and charge every organelle membrane for a duration which is dependent on both the charging time constant of the cell's plasma membrane as well as that of the organelle membrane [15].

The second critical nsPEF parameter is the amplitude of the pulse. Both the force exerted on charges and the electroporation of lipid membranes depend on the strength of the electric field. When the electric field across a cellular membrane exceeds about 1 V (2 kV/cm for a cell 10 μm in diameter), water-filled pores form in the membrane's lipid bilayer and the size and lifetime of these pores are dependent on the strength and duration of the electric field pulse. For amplitudes exceeding 2 kV/cm and pulse durations in the millisecond range, large pores form resulting in electroporation of the membrane that has been used to introduce normally impermeant anticancer drugs into targeted tissues [3–5,16]. For these long pulses, the pulse amplitude is limited to about 2 kV/cm to avoid thermal effects. Since heating is proportional to pulse duration and the square of the field strength, the much shorter pulses in the nanosecond range can have a higher field strength while delivering the same low level of thermal energy to the tissue. Here, we use a 20-fold higher field strength of 40 kV/cm and this generates structural changes in the plasma membrane that result in a smaller electrical barrier as well as higher voltage gradients across cellular organelles for the duration of the pulse [17]. A typical tumor cell nucleus measuring 10 μm in diameter will experience a voltage gradient of roughly 40 V across its diameter during each pulse. This electric field is large enough to cause electrodeformation [18].

Methods

Cell tissue culture

Murine melanoma B16-F10 cells were obtained from ATCC (Manassas, VA) and were stored frozen in liquid nitrogen until needed. They were thawed in a 37 °C water bath and then transferred to a culture flask containing DMEM (Dulbecco's modified Eagle's medium) supplemented with 10% fetal bovine serum (FBS, Atlanta Biologicals), 4 mM L-Glutamine (Cellgro), and 2% Penicillin–Streptomycin solution (Cellgro). The cells were grown in a 5% CO_2/95% air/100% humidified incubator at 37 °C.

Melanoma induction

Two to four tumors were induced in 120 female SKH-1 mice (immunocompetent, hairless, albino strain, Charles River, Wilmington, MA) by injecting 2–10 μl containing 10^6 B16-F10 murine melanoma cells just under the skin in the loose areolar tissue. A melanoma tumor can be seen at the injection site within a few days. Within 5 days the tumor is typically 3 mm wide and has exhibited angiogenesis. Untreated tumors typically grow to 10 mm wide or more within

a few weeks. For all animal studies the mice were kept under inhalation anesthesia using 1.6% isoflurane in oxygen. Tumors in animals #4 to #63 were treated with a 5-needle electrode array and #64 to #120 were treated with parallel plate electrodes. In a typical experiment, two tumors were used as controls and two others on the same mouse were treated with nsPEF.

In vivo imaging

Melanomas were imaged daily by both transillumination and surface photography at 1.2× magnification and ultrasound images were also taken beginning with mouse 50. Visualsonics Vevo 770 (Visualsonics Inc., Toronto, Canada) was used to image tumors in vivo. We used their model 708 scan head at 55 MHz with a stepper motor scanner providing a spatial resolution of 30 μm. The power Doppler mode provided blood flow images for each tumor.

Histology

Phosphate-buffered formalin (10%) was injected into the loose areolar layer under the skin at the tumor site immediately after euthanizing the mouse and 15 min prior to tumor dissection. The tumor was placed in formalin fixative (minimum 20× tumor volume) for 24–48 h at room temperature. The tumor and surrounding skin were trimmed and both external and internal surfaces were photographed. The fixed tumor was dehydrated through a standard 30%, 50%, 70%, 80%, 90%, 95%, and 100% X3 ethanol series, cleared in 100% X2 xylene, infiltrated at 60 °C in molten paraffin baths X2 (all for 1 h each), and then embedded in a paraffin block. Seven micrometer thick sections were cut and stained with hematoxylin and eosin.

Pulse generator

We used a pulse-forming network with an impedance of 75 Ω. It consists of 30 pairs of high voltage capacitors and 30 inductors arranged in a Blumlein configuration, and generates a 300 ns long high voltage pulse [19] (Fig. 1). The pulse was originally triggered by means of a spark gap that was later replaced by a mercury displacement relay controlled by a microcontroller. The voltage across the object was monitored using a high voltage probe (P6015A, Tektronix, Beaverton, CA), and the current was measured by means of a Pearson coil (model 2877, Pearson Electronics Inc., Palo Alto, CA). Current and voltage were recorded simultaneously using a digitizing oscilloscope (TDS3052, Tektronix, Beaverton, OR).

Electrodes for electric field application

We used two types of electrodes, a 5-needle array and parallel plates. The needle array (Fig. 2) was made using 30 gauge hypodermic needles (300 μm diameter) extending 2 mm from a Teflon base. The center needle was the anode and the four surrounding needles spaced 4 mm from the center electrode were connected together forming the cathode. The skin was coated with vegetable oil prior to needle insertion to increase the breakdown field strength along the skin and reduce the likelihood of flashover between needles during the pulsed field application. The parallel plate electrodes (Fig. 6A) were made from stainless steel with diameters of 3–5 mm, depending on the size of the tumor being treated. We coated these electrodes with a 0.5 mm thick layer of conductive agar (1 M NaCl in 2% agar) to separate the skin from the electrode. For treatment, each tumor was positioned between two plates with a separation of 0.5–1 mm, while 100 pulses 300 ns in duration and 4–8 kV in amplitude with a rise time of about 30 ns were applied at a frequency of 0.5 Hz.

Determination of caspase activation in vitro

Caspase activity was determined in vitro from melanoma tumor extracts after exposure to nsPEF. Melanomas were dissected out of the mouse and frozen in liquid nitrogen. Extracts were prepared from thawed tissue homogenates and assayed for caspase activity using the fluorogenic substrate Ac-DEVD-AFC (Alexis Biochemicals, San Diego, CA) as previously

described [20]. This peptide sequence is based on the PARP cleavage site, Asp^{216}, for caspases 1, 3, 4, and 7, that exhibits enhanced fluorescence upon cleavage. Briefly, extracts were incubated with 50 μM DEVD-AFC (Asp-Glu-Val-Asp-AFC) and fluorescence (excitation 400 nm and emission 505 nm) was determined. Caspase units were defined as picomoles of substrate cleaved per minute per milligram extract protein.

Results and discussion

The electric field was applied using two different electrode configurations. The first was a 5-needle electrode array (Fig. 2A) in which the needles penetrated about 2 mm into the mouse skin. In 59 mice, the central needle was placed in the center of the melanoma to be treated and the outer four needles were outside of the boundary edges of the melanoma. This electrode array exhibits a sharply non-uniform field with field lines parallel to the surface of the skin and strongest near the center electrode (Fig. 2B). When the needle array is inserted into a melanoma for a couple of minutes and removed, the melanoma continues to grow normally (Figs. 3H–M). However, if 100 pulses (8 kV, 300 ns, 0.5 Hz) are administered to the needle array prior to removal, the melanoma begins to shrink within 2 days (Figs. 3O–T). Blood flow to the tumor is disrupted after pulsing as red blood cells leak out of capillaries surrounding the tumor (Fig. 3P). Local blood flow usually does not recover for about two weeks. Two days after pulsing, the stratum corneum shows signs of necrosis and hemorrhage with accompanying superficial erosion of the epidermis and the tumor becomes darker (Fig. 3Q). This suggests that in addition to the tumor cells, the epidermal cells of the skin between the electrodes that differentiate into the stratum corneum are damaged by the 300 ns pulsed electric field (nsPEF). We confirmed this by treating skin regions where there were no melanomas and observing similar superficial erosion over the same time period (Figs. 3A–F). Insulating the upper shaft of the needles that come into contact with the epidermis may reduce this damage.

This tumor response is dependent on both field strength and pulse number. If the field strength is cut in half by using a 4 kV pulse (average field of 10 kV/cm), there is no significant difference between the growth rates of treated and control tumors (Fig. 4A). This holds true for the application of both 10 and 100 pulses (Fig. 4B). The pulse number dependence is more evident for the 8 kV pulses (20 kV/cm field) where the response is stronger for 100 pulses than it is for 10 (Figs. 4C and D) and even stronger when two treatments of 100 pulses are given (Fig. 4E). Under this latter condition, the tumors shrink by about 75% within 8 days.

The second electrode configuration used involved placing the tumor between two parallel plates (Fig. 6A). The electric field between two parallel plates is uniform except at the edges, so that all cells between the plates will be exposed to the same field strength. These electrodes were used when treating 48 mice by lifting a fold of skin containing the melanoma away from the mouse and placing it between the electrodes in such a way that the entire tumor was positioned between the plates. Thus, the field was oriented perpendicular to the skin surface rather than parallel to it as with the needle electrodes. The distance between the plates was typically 0.5–1 mm, depending on tumor thickness. Based on our previous results with needle electrodes, we used a field strength of 40 kV/cm and the typical response to nanosecond pulses with this electrode configuration is illustrated in Fig. 5. One difference between the two electrode types is the appearance of the skin beginning two days after treatment. A black scab appears on the stratum corneum in the pulsed region and it remains for about two weeks as the stratum corneum is regenerated (Fig. 5B). Histological examination of this scab indicates that it is composed of clotted red blood cells. Tumors typically shrank by 90% within two weeks following four 100-pulse treatments using plate electrodes (3 on day 0 and 1 on day 4) (Fig. 6B). However after about two weeks of regression, all tumors began to grow again and we sacrificed the mice at that time so that we could fix and section the tumors for histology.

Multiple treatments result in complete tumor remission

We have begun to treat tumors with a second 3-day series of 100 pulses when they stop shrinking two to three weeks after the initial treatment. In three completed cases now, we have observed total remission of the tumor and one example is shown in Fig. 7. Within two months of the initial treatment, the melanoma was undetectable by transillumination, ultrasound or serial section histological investigation. We believe that further optimization of the nsPEF parameters should make it possible to routinely eliminate these skin tumors at a high rate of efficacy.

nsPEF raises tumor temperature only 3 °C

The energy delivered to the tissue between 5 mm plates is 0.2 J if the plate separation is 1 mm. Given the specific heat of water, this should only increase the tissue temperature by two to three degrees. We directly measured this temperature increase by inserting a very small thermocouple into the tumor and confirmed that the maximum temperature reached after 100 pulses was 33 °C (Fig. 8). This is ten degrees lower than the minimum temperature required for hyperthermia effects so it is very unlikely that effects of nsPEF on tumor growth are due to hyperthermia.

Targets and potential mechanisms for nsPEF effects

We have identified two immediate changes in the tumor following the application of the electric field pulses that may be responsible for the tumor regression: (1) tumor cell nuclei rapidly become pyknotic and (2) blood stops flowing to the tumor. Untreated tumor cells exhibited lightly staining pleomorphic nuclei and abundant cytoplasm containing finely dispersed melanin granules (Fig. 9). Treated tumors exhibited dense staining, shrunken nuclei, and dyshesion of individual cells with coarse intracellular melanin granules as well as aggregated extracellular melanin granules in the widened interstitial spaces. The tumor cell nuclei shrink by 54% within a few minutes after pulsing and by 68% within 3 h. No further nuclear shrinkage occurred during the subsequent two weeks as the tumor decreased in size by 90% (Fig. 9E). Some of the tumor nuclei elongate along the electric field axis but this is not always observed. The tumor cells themselves also shrink over this time period because the cell density is higher by one and three hours post-treatment. The nuclear pyknosis that follows pulse application occurs faster than any previously observed pyknotic response [21] and may result from either electrodeformation [18] or the direct electric field interaction with cytoskeletal elements associated with the cell's nuclear lamina to generate the nuclear elongation and shrinking [22,23].

The second major change that is immediately obvious is a reduction in blood flow to the tumor. Both transillumination and power Doppler ultrasound reconstructions indicate that the blood flow has stopped within about 15 min after pulsing (Fig. 10). Histology confirms that red blood cells are found scattered within and around the melanoma tumor. This implies that the local blood vessels become leaky and red blood cells escape into the surrounding tissues. Blood flow to the tumor does not normally recover for about two weeks. If blood flow returns, the tumor usually begins growing again. This lack of blood flow to the melanoma certainly contributes to its regression.

We also looked for changes in the classical apoptosis marker, caspase activity. We measured the activity of caspases using a fluorogenic substrate Ac-DEVD-AFC at 0, 3, 6, and 9 h after treatment with 100 pulses in three experiments. The only time at which caspase activity appeared to increase was at 3 h when there was a 2.6-fold increase in mean activity. However, this small change failed the normality t test and the Mann–Whitney Rank Sum test indicating that it was not a statistically significant difference ($p = 0.1$). It is possible that an apoptosis

program is initiated, but since apoptosis is an energy-requiring process, the interruption of the blood supply to the tumor may prevent completion of the apoptosis mechanism.

Previously reported changes in DNA post-nsPEF

The rapid pyknosis that we observe suggests that the cellular DNA could be a direct or indirect target of nsPEF. Three previous studies provided direct evidence for this. (1) Using a comet assay, Stacey et al. [24] found that ten 60 ns pulses of 60 kV/cm caused a rapid 2.6-fold increase in the mean image length of DNA electrophoresis tracks in Jurkat cell extracts and a 1.6-fold increase in the comet assay from HL60 cell extracts. In both cases, this was a very significant change ($p < 0.001$). This elongation in DNA electrophoresis tracks is normally interpreted to indicate fragmentation of the DNA into smaller pieces that is associated with apoptotic cell death. (2) Tseng's group [25] has been using human whole genome microarrays with 55,000 different gene probes to analyze the effects of nsPEF on Jurkat cells. They found 55 genes with increased expression at 30 or 60 min following exposure to two consecutive 10 ns pulses of 280 kV/cm. The interesting correlation is that most of these genes were involved in DNA repair, cell cycle arrest, and transcription repression. Up-regulation of DNA repair genes is consistent with the DNA fragmentation observed by Stacey as discussed above. (3) A third indication of changes in the DNA following nsPEF treatment comes from images of the nucleus labeled with acridine orange, a vital fluorescent dye that intercalates into DNA and RNA [26]. A single 10 ns pulse of 26 kV/cm caused a dramatic decrease in fluorescence intensity in the nucleus evident as early as 5 min after the pulse. This change could be due to an outflow of DNA or to conformational changes in the DNA.

These three observations using three different techniques from three different laboratories all support the hypothesis that nsPEF can produce DNA damage. The precise mechanism by which this damage is induced is not clear. Two possible mechanisms include activation of DNases in the apoptotic pathway or mechanically induced DNA breakage. A typical tumor cell nucleus measuring 10 μm in diameter will experience a voltage gradient of about 40 V across itself during each pulse. This electric field is large enough to cause rapid electromechanical deformation of the nucleus [18,22] generating a mechanical shock to the DNA attached to the nuclear envelope that could damage the DNA.

These nsPEFs stimulate murine melanomas to self-destruct by triggering rapid pyknosis and reducing blood flow without significant increases in caspase activity. A reduction in blood flow to tumors has also been observed following electrochemotherapy but does not occur until 24 h after treatment when the bleomycin entry had destroyed the endothelial cells [27]. In contrast, nsPEF requires no drugs to achieve this dramatic reduction in tumor blood flow. This cellular response to a new nanosecond time domain of pulsed electric field application is both novel and deadly. While we have not yet tested this technique on humans, we feel that it may have advantages over the surgical removal of skin lesions because incisions through the dermis often leave scarring on the healed skin. nsPEFs affect the tumor without disrupting the dermis so that scarring is less likely. nsPEFs should also be effective on other tumor types located deeper in the body if a catheter electrode can be guided to the tumor. This highly localized and drug-free physical technique offers a promising new therapy for tumor treatment.

Acknowledgements

We thank Richard Heller for suggesting the use of the murine B16 melanoma cell line for testing the effects of nsPEFs on tumors. This work was supported by grants from the Air Force Office of Scientific Research, American Cancer Society, Old Dominion University, BioElectroMed Corp., a gift from Mr. Frank Reidy, and with internal funds of the Frank Reidy Research Center for Bioelectrics at Old Dominion University.

References

1. Tanabe KK, Curley SA, Dodd GD, Siperstein AE, Goldberg SN. Radiofrequency ablation: the experts weigh in. Cancer 2004;100:641–650. [PubMed: 14745883]
2. Haemmerich D, Laeseke PF. Thermal tumour ablation: devices, clinical applications and future directions. Int J Hyperthermia 2005;21:755–760. [PubMed: 16338858]
3. Lucas ML, Heller R. IL-12 gene therapy using an electrically mediated nonviral approach reduces metastatic growth of melanoma DNA. Cell Biol 2003;22:755–763.
4. Kubota Y, Tomita Y, Tsukigi M, Kurachi H, Motoyama T, Mir LM. A case of perineal malignant melanoma successfully treated with electrochemotherapy. Melanoma Res 2005;15:133–134. [PubMed: 15846147]
5. Gothelf A, Mir LM, Gehl J. Electrochemotherapy: results of cancer treatment using enhanced delivery of bleomycin by electroporation. Cancer Treat Rev 2003;29:371–387. [PubMed: 12972356]
6. Beebe SJ, Fox P, Rec LJ, Somers K, Stark RH, Schoenbach KH. Nanosecond pulsed electric field (nsPEF) effects on cells and tissues: apoptosis induction and tumor growth inhibition. IEEE Trans Plasma Sci 2002;30:286–292.
7. Schoenbach KH, Beebe SJ, Buescher ES. Intracellular effect of ultrashort electrical pulses. Bioelectromagnetics 2001;22:440–448. [PubMed: 11536285]
8. Buescher ES, Schoenbach KH. Effects of submicrosecond, high intensity pulsed electric fields on living cells-intracellular electromanipulation. IEEE Trans Dielect El In 2003;10:788–794.
9. Vernier PT, Sun YH, Marcu L, Salemi S, Craft CM, Gundersen MA. Calcium bursts induced by nanosecond electric pulses. Biochem Biophys Res Commun 2003;310:286–295. [PubMed: 14521908]
10. Buescher ES, Smith RR, Schoenbach KH. Submicrosecond intense pulsed electric field effects on intracellular free calcium: mechanisms and effects. IEEE Trans Plasma Sci 2004;32:1563–1572.
11. White JA, Blackmore PF, Schoenbach KH, Beebe SJ. Stimulation of capacitative calcium entry in HL-60 cells by nanosecond pulsed electric fields. J Biol Chem 2004;279:22964–22972. [PubMed: 15026420]
12. Beebe SJ, Fox PM, Rec LJ, Willis EL, Schoenbach KH. Nanosecond, high-intensity pulsed electric fields induce apoptosis in human cells. FASEB J 2003;17:1493–1495. [PubMed: 12824299]
13. Beebe SJ, White J, Blackmore PF, Deng Y, Somers K, Schoenbach KH. Diverse effects of nanosecond pulsed electric fields on cells and tissues DNA. Cell Biol 2003;22:785–796.
14. Beebe SJ, Blackmore PF, White J, Joshi RP, Schoenbach KH. Nanosecond pulsed electric fields modulate cell function through intracellular signal transduction mechanisms. Physiol Meas 2004;25:1077–1093. [PubMed: 15382843]
15. Schoenbach KH, Joshi RP, Kolb JF, Chen N, Stacey M, Blackmore PF, Buescher ES, Beebe SJ. Ultrashort electrical pulses open a new gateway into biological cells. Proc IEEE 2004;92:1122–1137.
16. Teissie J, Golzio M, Rols MP. Mechanisms of cell membrane electropermeabilization: a minireview of our present (lack of ?) knowledge. Biochim Biophys Acta 2005;1724:270–280. [PubMed: 15951114]
17. Hu Q, Viswanadham S, Joshi RP, Schoenbach KH, Beebe SJ, Blackmore PF. Simulations of transient membrane behavior in cells subjected to a high-intensity, ultra-short electric pulse. Phys Rev E Stat Nonlin Soft Matter Phys 2005 031914–031921;71:031914–9. [PubMed: 15903466]
18. Joshi RP, Hu Q, Schoenbach KH, Hjalmarson HP. Theoretical predictions of electromechanical deformation of cells subjected to high voltages for membrane electroporation. Phys Rev E Stat Nonlin Soft Matter Phys 2002;65:021913. [PubMed: 11863569]
19. J.F. Kolb, S. Kono, K.H. Schoenbach, Nanosecond pulsed electric field generators for the study of subcellular effects, Bioelectromagnetics (2006), in press.
20. Parvathenani LK, Buescher ES, Chacon-Cruz E, Beebe SJ. Type I cAMP-dependent protein kinase delays apoptosis in human neutrophils at a site upstream of caspase-3. J Biol Chem 1998;273:6736–6743. [PubMed: 9506973]
21. Albarenque SM, Doi K. T-2 toxin-induced apoptosis in rat keratinocyte primary cultures. Exp Mol Pathol 2005;78:144–149. [PubMed: 15713441]
22. Wong PK, Tan W, Ho CM. Cell relaxation after electrodeformation: effect of latrunculin A on cytoskeletal actin. J Biomech 2005;38:529–535. [PubMed: 15652551]

23. Gruenbaum Y, Margalit A, Goldman RD, Shumaker DK, Wilson KL. The nuclear lamina comes of age. Nat Rev Mol Cell Biol 2005;6:21–31. [PubMed: 15688064]

24. Stacey M, Stickley J, Fox P, Statler V, Schoenbach K, Beebe SJ, Buescher S. Differential effects in cells exposed to ultra-short, high intensity electric fields: cell survival, DNA damage, and cell cycle analysis. Mutat Res 2003;542:65–75. [PubMed: 14644355]

25. Z.M. Wang, X. Ge, S.M. Wang, A. Bassi, M. Khalid, K.H. Schoenbach, C.Q. Zhou, H.L. Gerber, C.C. Tseng, Early response genes to DNA damage by nanosecond pulsed electric fields, IEEE Trans. Plasma Sci. (2006), in press.

26. Chen N, Schoenbach KH, Kolb JF, James SR, Garner AL, Yang J, Joshi RP, Beebe SJ. Leukemic cell intracellular responses to nanosecond electric fields. Biochem Biophys Res Commun 2004;317:421–427. [PubMed: 15063775]

27. Sersa G, Cemazar M, Parkins CS, Chaplin DJ. Tumour blood flow changes induced by application of electric pulses. Eur J Cancer 1999;35:672–677. [PubMed: 10492645]

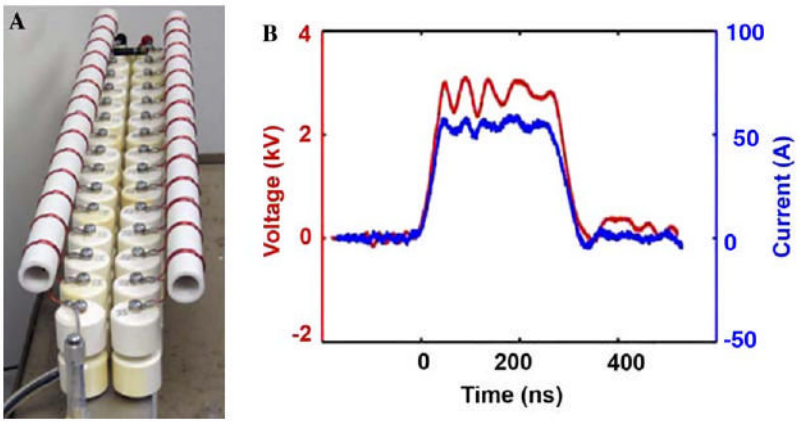

Fig. 1.

Pulse generator used in these experiments. (A) Three hundred nanosecond pulse-forming network in Blumlein configuration. Width of each ceramic capacitor is 3 cm. (B) Typical voltage (red or solid trace) and current (blue or dashed trace) pulse generated across a tumor (for interpretation of the reference to color in this figure legend, the reader is referred to the web version of this paper).

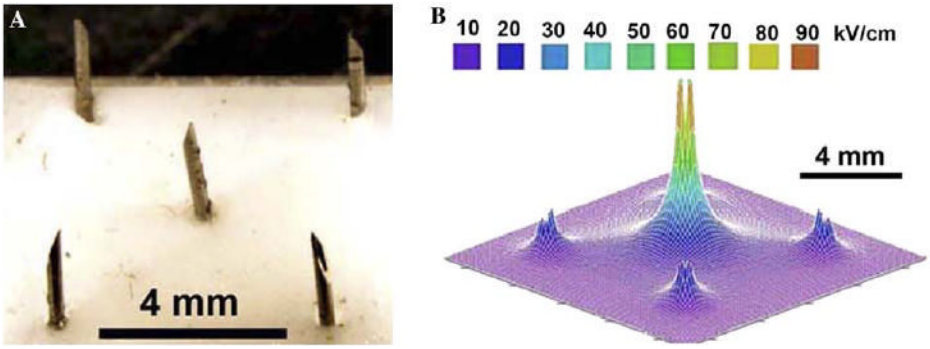

Fig. 2.

Needle array electrode and electric field pattern. (A) Photograph of 5-needle array used for the first experiments. (B) 3-D plot of the electric field generated when 8 kV is placed on the center electrode and the outer four electrodes are held at ground.

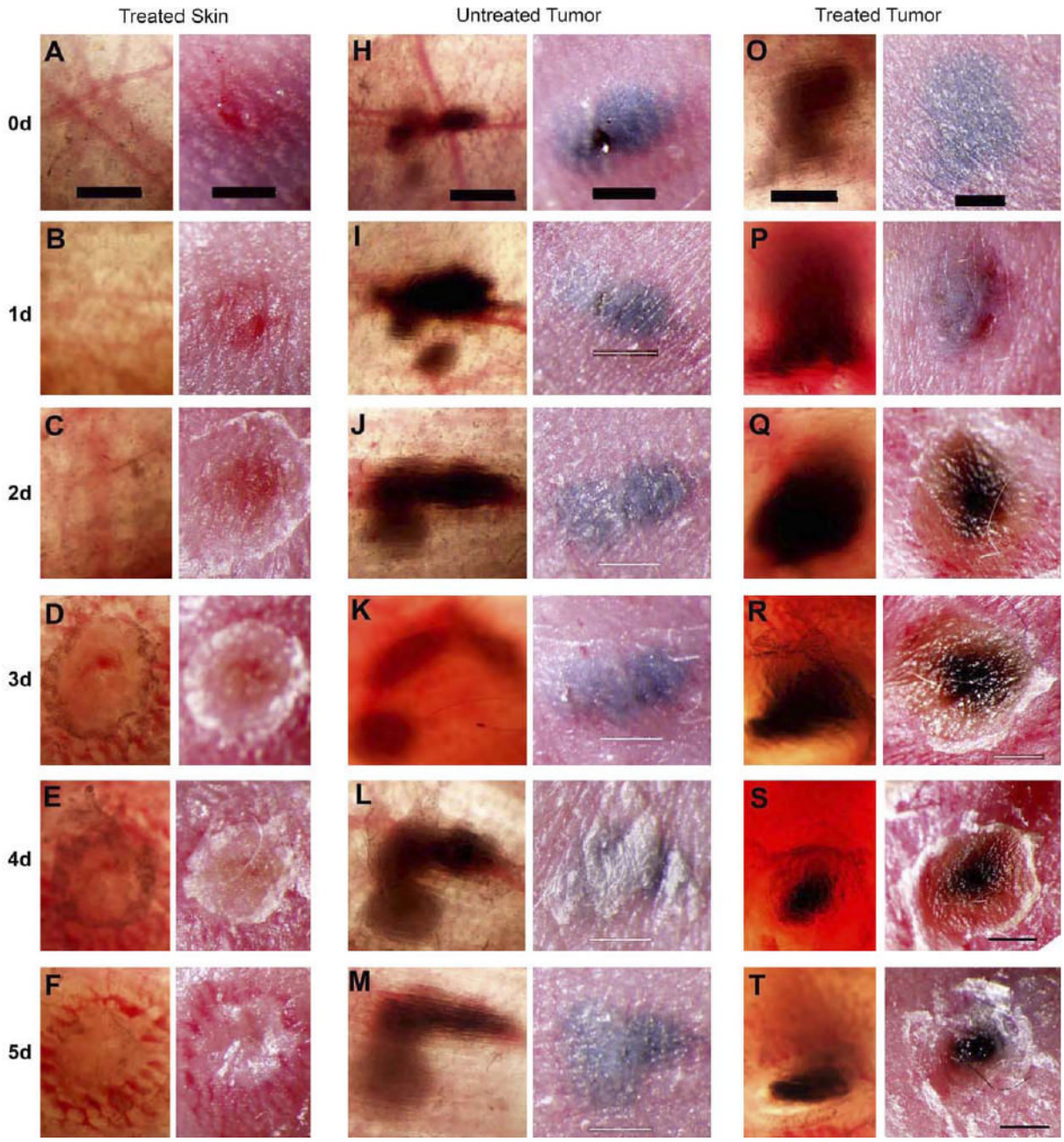

Fig. 3.

Typical response of skin and melanoma to one or two applications of 100 pulses using a 5-needle array electrode on mouse #56. Each matched pair of photographs represents an in vivo transillumination of the skin on the left and a surface view on the right. Numbers on the far left indicate the number of days after pulsing at which all three matched pairs to the right were photographed. (A–F) The typical response of normal skin to 100 pulses (300 ns long, 20 kV/cm, 0.5 Hz) delivered on day 0. Small superficial erosion in (B) grows in (C–E) and indicates loss of some or all epidermis. (H–M) The electrode array was inserted into this tumor on day 0 but no pulses were delivered. (O–T) One hundred pulses (300 ns long, 20 kV/cm) were delivered at 0.5 Hz on day 0 and day 1. Necrosis evident on day two becomes more intense

over time. Scale bars (A–T) 1 mm and all photographs in a given row are at the same magnification.

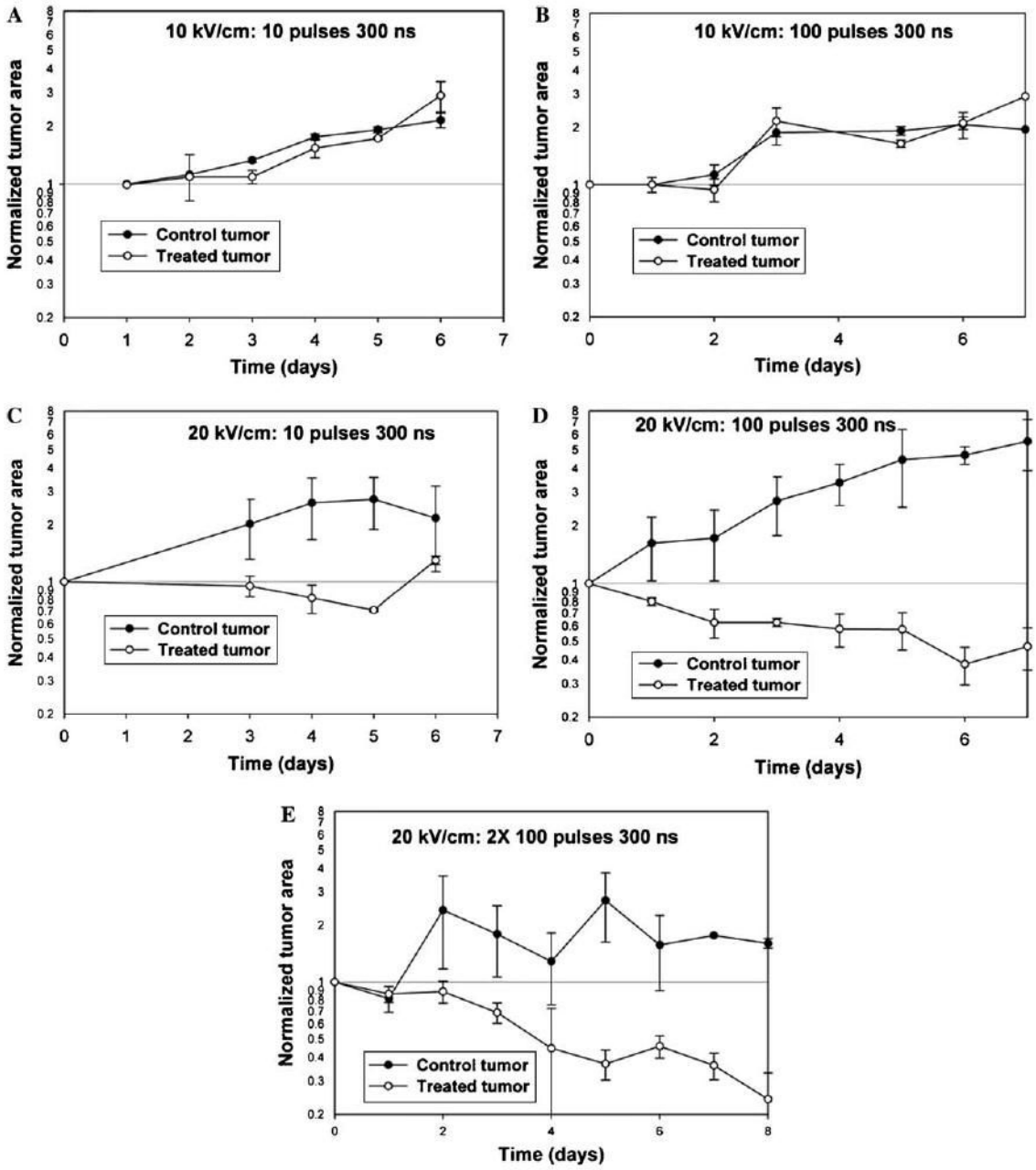

Fig. 4.

Summary of the size changes in a total of 23 melanomas after the indicated treatments using the 5-needle array. For each day the tumor area was measured from the transillumination image and divided by that measured on day zero to give the normalized area. The average response of two to three tumors from different animals is plotted on a logarithmic scale and the error bars represent the SEM. Pulses were applied at a frequency of 0.5 Hz. (A, B) 4 kV was applied between center and outer needles spaced 4 mm apart to give an average field of 10 kV/cm. (C–E) Eight kilovolt was applied between the center and outer needles to give an average field of 20 kV/cm.

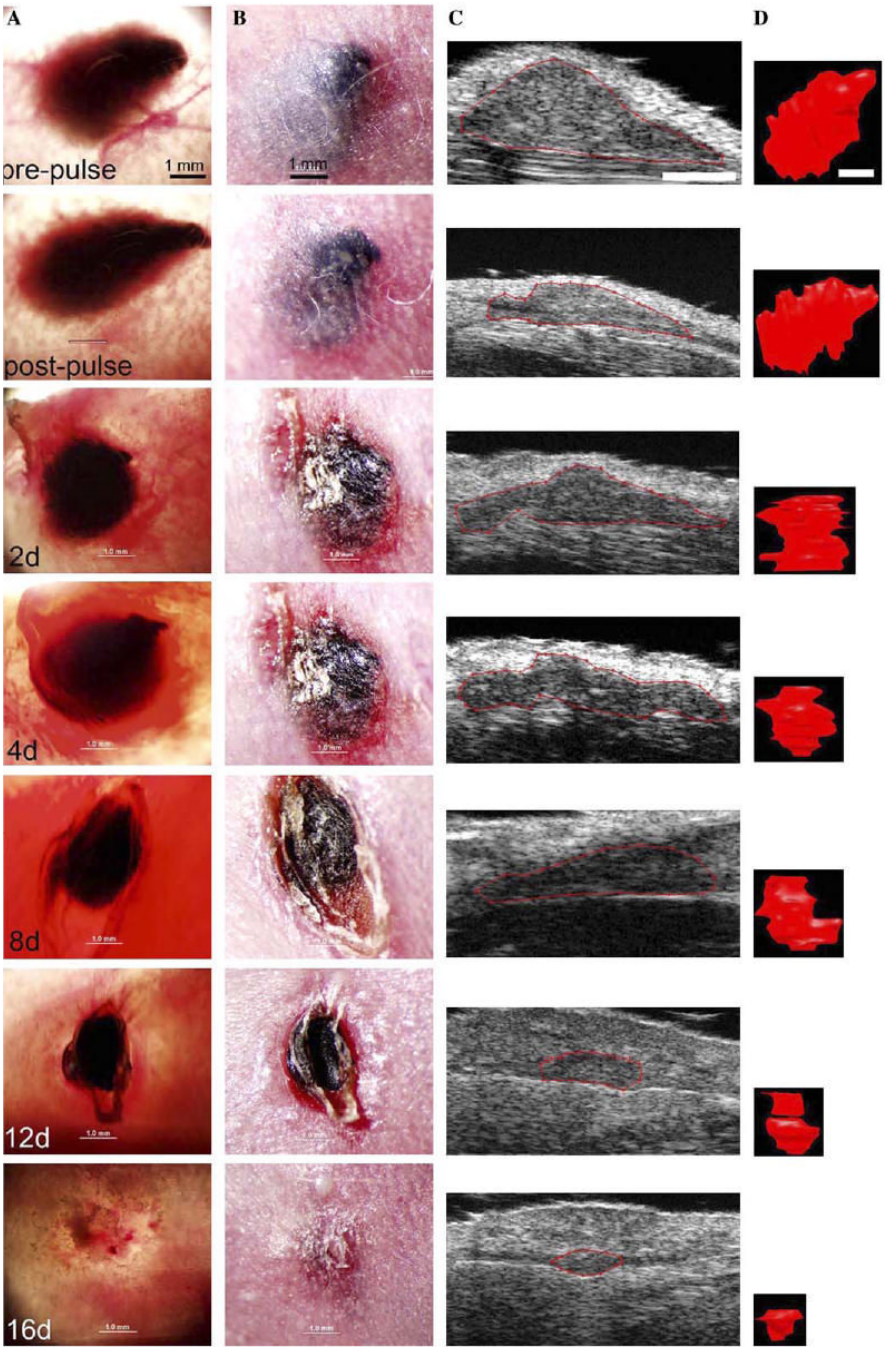

Fig. 5.

Typical response of a melanoma to three applications of 100 pulses (300 ns, 40 kV/cm, 0.5 Hz) 30 min apart on day 0 followed by a single application on day 4 using a 5 mm diameter parallel plate electrode on mouse #102. Collection of seven matched sets of images of the same tumor all taken on the day indicated in the lower left corner of the transillumination image. (Column A) Transillumination image. (Column B) Surface view. (Column C) Ultrasound slice at center of tumor; (column D) 3-D reconstruction made from 100 serial ultrasound slices through tumor. Magnification is constant for each column and scale bar at top of each column represents 1 mm.

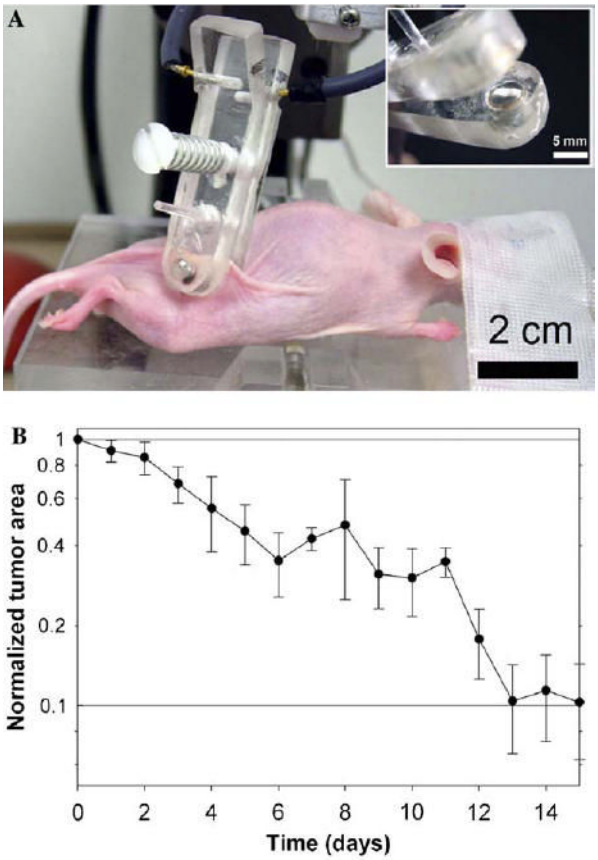

Fig. 6.

(A) Photograph of SKH-1 hairless mouse being treated with parallel plate electrode under isoflurane inhalation anesthesia. (Inset) Close-up of one of the plates of parallel plate electrode showing it recessed by 0.5 mm to allow a space for a conductive agar gel to be placed on it. (B) Mean change in normalized area of the transillumination image of six tumors from three mice treated with parallel plate electrodes using the same 4 × 100 pulse applications (3 × 100 on day 0 and 1 × 100 on day 4). 40–80 kV/cm, 300 ns pulses at 0.5 Hz. Error bars indicate the SEM.

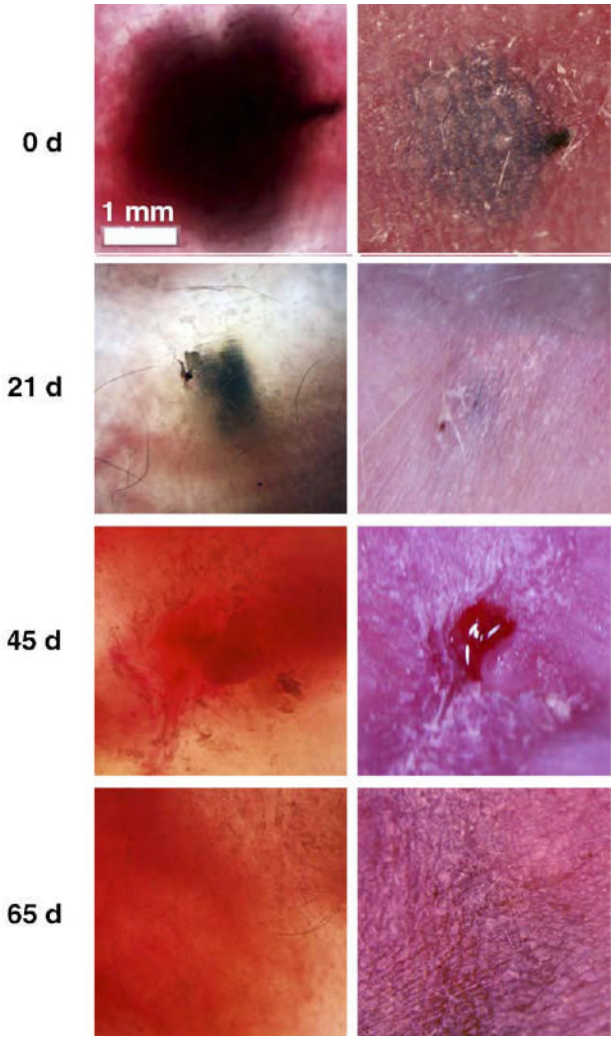

Fig. 7.

Complete regression of melanoma evident by 65 days after the first treatment. One hundred pulses of 300 ns and 40 kV/cm were applied on days 0, 1, 2 and 21, 22, 23. Each pair of photographs were taken on the day indicated at the left; transillumination on left and surface view on right. The scale bar in upper left represents 1 mm and is the same for all images.

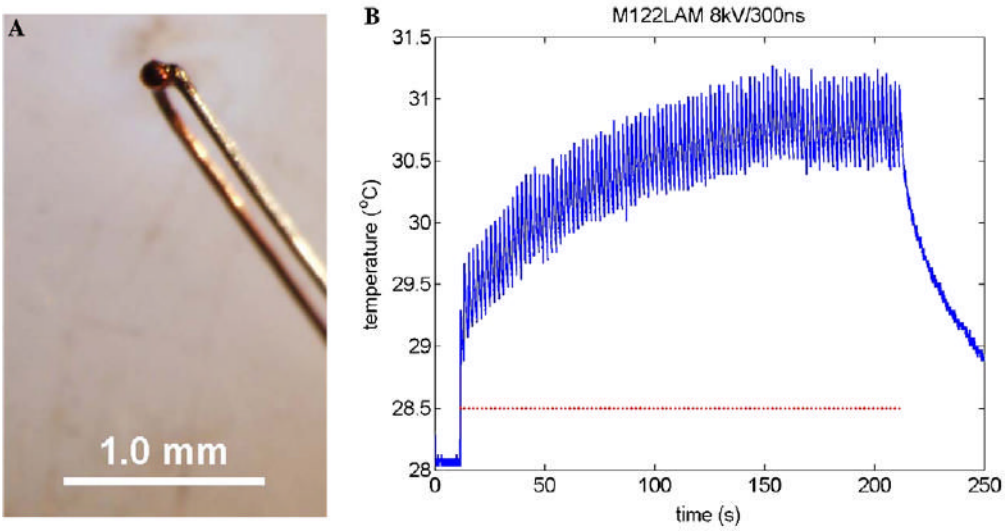

Fig. 8.

Measurement of the temperature within a melanoma during nsPEF application. (A) Micrograph of a thermocouple made by fusing a copper wire with one made from constantine. (B) Temperature record from a thermocouple positioned inside of a melanoma during pulse application. Lower dots indicate the time that each pulse was applied.

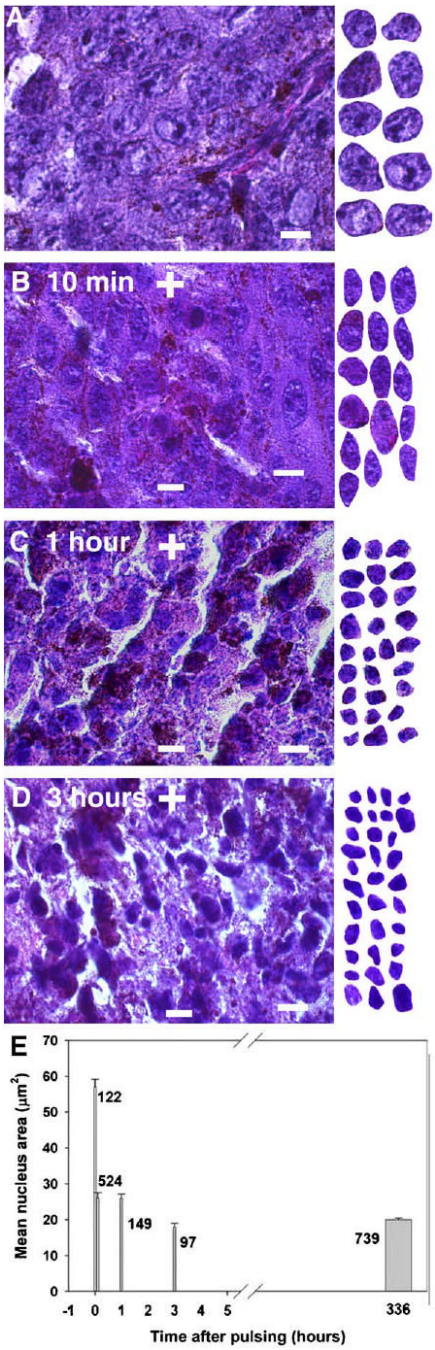

Fig. 9.

Targets and mechanisms of nsPEF effects. (A–D) Seven micrometer thick paraffin sections of control and treated melanomas fixed at the indicated time after treatment with 100 pulses (300 ns, 40 kV/cm, 0.5 Hz) stained with hematoxylin and eosin. The clearest nuclei were copied and placed to the right of each section to assist in size comparison. (A) Control tumor section; (B) 10 min post-treatment (C) 1 h post-treatment. (D) Three hours post-treatment. Scale bars: 10 μm. (E) Mean nuclear area versus time after 100–200 pulses were applied. Number of cell nuclei measured from at least two mice for each time point indicated next to each column and bars represent SEM. Breakin time is 330 h. There is a significant difference between the 0 h

prepulse control and all of the other time points ($p < 0.001$) as well as between 1 and 3 h ($p < 0.001$). There is no significant difference between 0.1 and 1 h. Scale bars in (A)–(D): 10 μm.

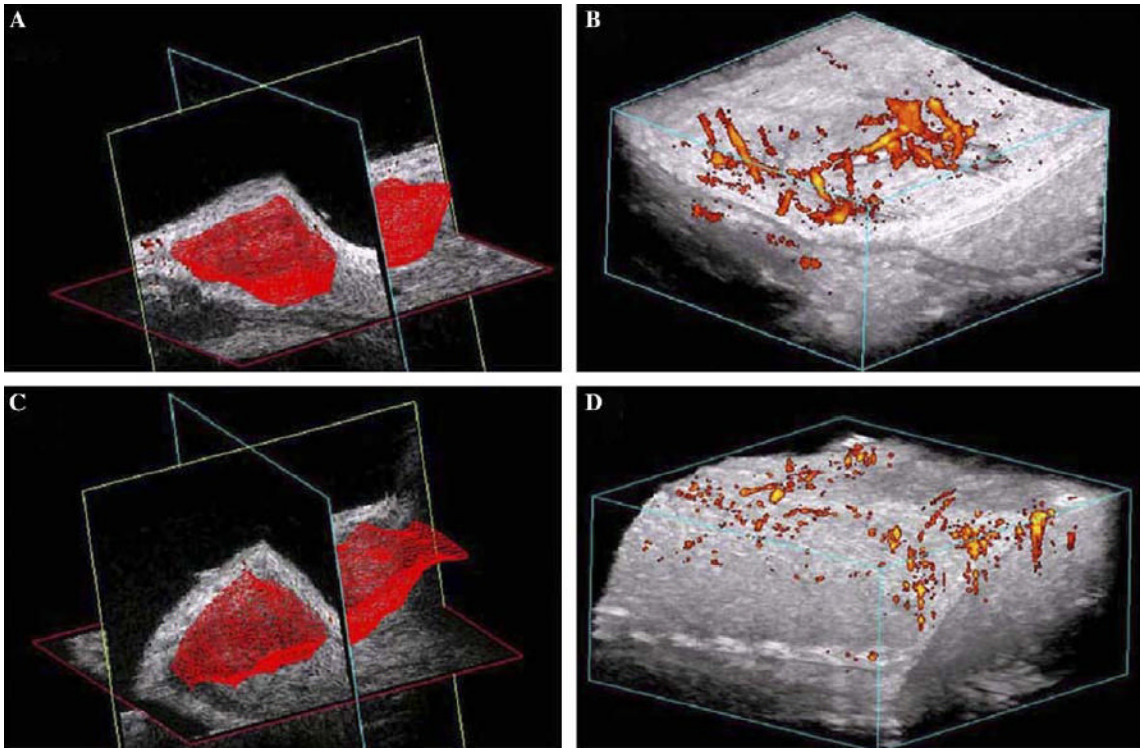

Fig. 10.

Blood flow in melanoma before and after nsPEF application. (A) 3-D reconstruction of volume of melanoma; (B) power Doppler reconstruction of blood flow before field application. (C) 3-D reconstruction of volume of the same melanoma shown in (A) generated about 15 min after 100 pulses (300 ns, 40 kV/cm, 0.5 Hz). (D) Power Doppler reconstruction of blood flow in the same tumor shown in (B) generated about 15 min after 100 pulses (300 ns, 40 kV/cm, 0.5 Hz).